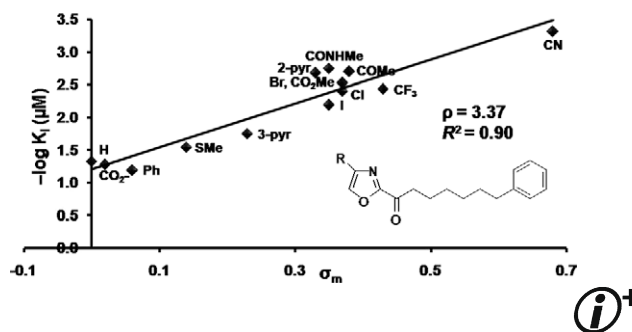




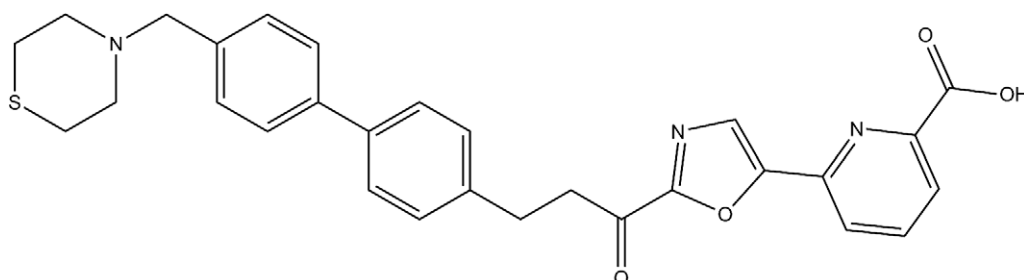
Chemical structure of THL (10-undecylnyl-3-methyl-2-oxo-1,3-dioxolane-5-carboxamide) is shown above the gel. The gel displays the effect of THL on the activity of FAAH, BAT5, KIAA1363, and ABHD12. Lanes are labeled with THL concentrations: -, 100, 50, 10, 2.5, 0.5, 0.1, and 0.01  $\mu\text{M}$ . The bands represent the products of the hydrolysis reaction, with the intensity of the bands indicating the activity of each enzyme. FAAH and BAT5 show a dose-dependent inhibition of activity by THL, while KIAA1363 and ABHD12 show no significant change in activity across the tested concentrations.



### Correlation of inhibitor effects on enzyme activity and thermal stability for the integral membrane protein fatty acid amide hydrolase

pp 5847–5850

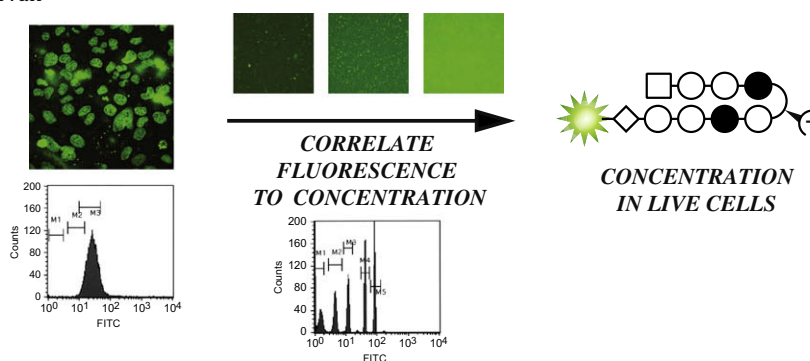
Ian M. Slaymaker, Michael Bracey, Mauro Mileni, Joie Garfunkle, Benjamin F. Cravatt, Dale L. Boger, Raymond C. Stevens\*



### Quantitating the concentration of Py-Im polyamide–fluorescein conjugates in live cells

pp 5851–5855

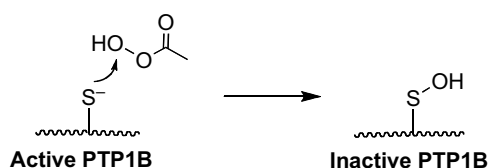
Carey F. Hsu, Peter B. Dervan\*



### Oxidative inactivation of protein tyrosine phosphatase 1B by organic hydroperoxides

pp 5856–5859

Sanjib Bhattacharya, Jason N. LaButti, Derrick R. Seiner, Kent S. Gates\*

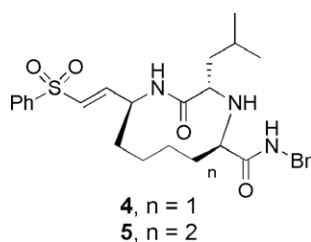


Protein tyrosine phosphatases (PTPs) are cysteine-dependent enzymes that play a central role in cell signaling. Organic hydroperoxides cause thiol-reversible, oxidative inactivation of PTP1B in a manner that mirrors the endogenous signaling agent hydrogen peroxide.

### Synthesis of macrocyclic trypanosomal cysteine protease inhibitors

pp 5860–5863

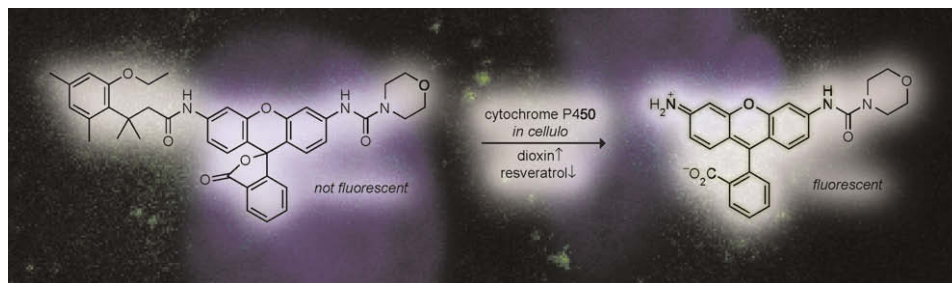
Yen Ting Chen, Ricardo Lira, Elizabeth Hansell, James H. McKerrow, William R. Roush\*



**A highly sensitive fluorogenic probe for cytochrome P450 activity in live cells**

pp 5864–5866

Melissa M. Yatzeck, Luke D. Lavis, Tzu-Yuan Chao, Sunil S. Chandran, Ronald T. Raines\*

**Synthesis and characterization of BODIPY-labeled colchicine**

pp 5867–5870

Leggy A. Arnold, Patricia Ranaivo, R. Kiplin Guy\*

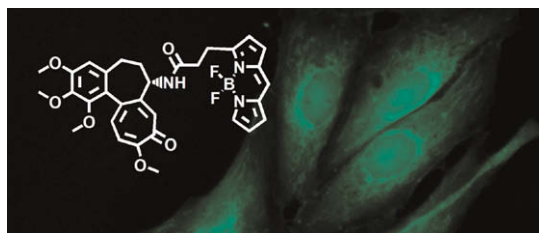
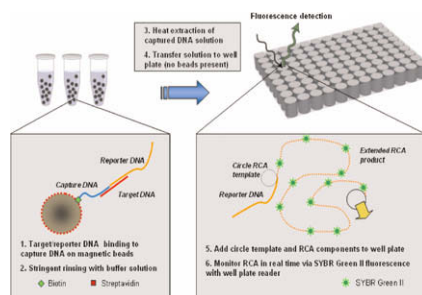


Photo-stable and pH-independent BODIPY-labeled colchicine analogs were synthesized to allow analysis of the cellular distribution of tubulin.

**Sensitive and selective viral DNA detection assay via microbead-based rolling circle amplification**

pp 5871–5874

Eric Schopf, Nicholas O. Fischer, Yong Chen, Jeffrey B.-H. Tok\*



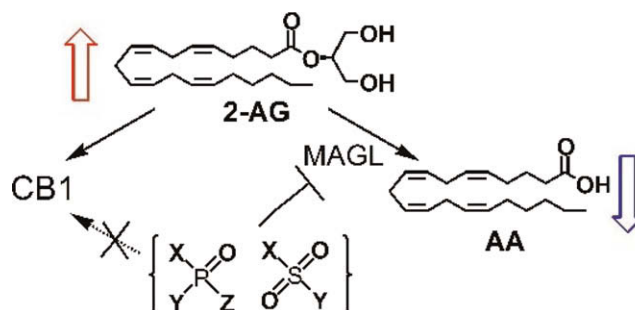
We report a sensitive and efficient magnetic bead-based assay for viral DNA identification using isothermal amplification of a reporting probe.

**Monoacylglycerol lipase regulates 2-arachidonoylglycerol action and arachidonic acid levels**

pp 5875–5878

Daniel K. Nomura, Carolyn S. S. Hudak, Anna M. Ward, James J. Burston, Roger S. Issa, Karl J. Fisher, Mary E. Abood, Jenny L. Wiley, Aron H. Lichtman, John E. Casida\*

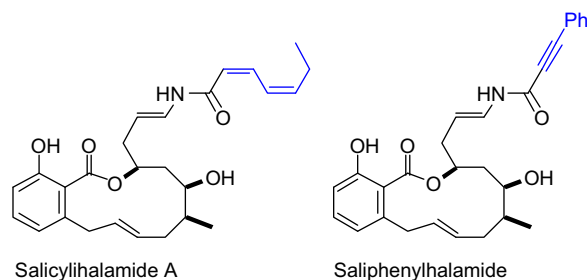
Potent MAGL inhibitors in mice elevate 2-AG and correspondingly lower AA levels in some but not in all tissues. Apparent direct OP displacement of CB1 agonist binding may be due instead to 2-AG in brain membranes which is metabolically stabilized by MAGL inhibition.



### Evaluating the potential of Vacuolar ATPase inhibitors as anticancer agents and multigram synthesis of the potent salicylilhalamide analog saliphenylhalamide

pp 5879–5883

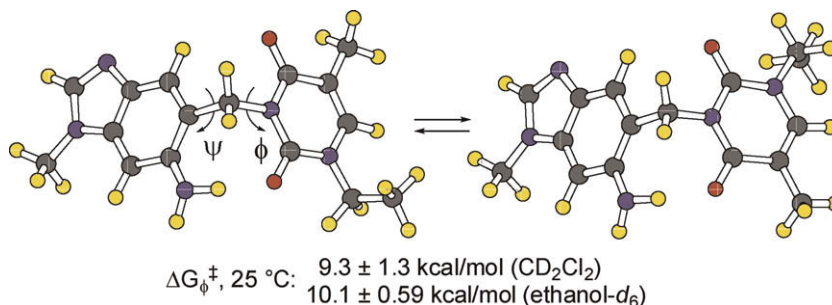
Sylvain Lebreton, Janis Jaunbergs, Michael G. Roth, Deborah A. Ferguson, Jef K. De Brabander\*



### Conformational analysis of a covalently cross-linked Watson–Crick base pair model

pp 5884–5887

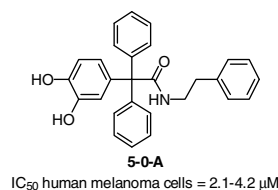
Erik A. Jensen, Benjamin D. Allen, Yoshito Kishi, Daniel J. O'Leary\*



### Triphenylmethalamides (TPMAs): Structure–activity relationship of compounds that induce apoptosis in melanoma cells

pp 5888–5891

Rahul Palchaudhuri, Paul J. Hergenrother\*



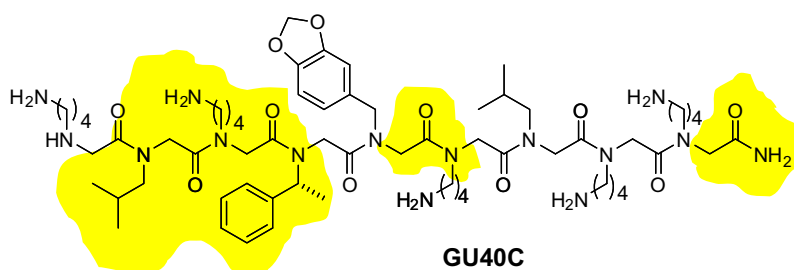
The optimization of triphenylmethalamides (TPMAs) as anticancer agents is reported.



### The pharmacophore of a peptoid VEGF receptor 2 antagonist includes both side chain and main chain residues

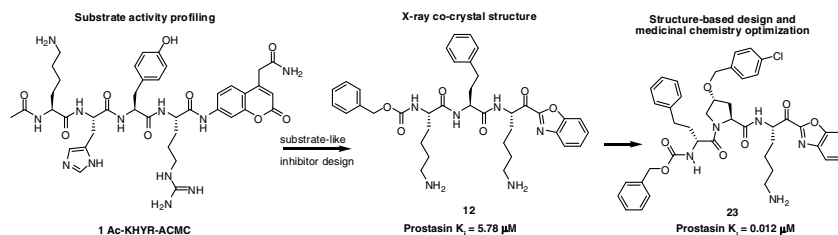
pp 5892–5894

D. Gomika Udugamasooriya, Geoff Dunham, Caroline Ritchie, Rolf A. Brekken, Thomas Kodadek\*



**Discovery of inhibitors of the channel-activating protease prostatic (CAP1/PRSS8) utilizing structure-based design** pp 5895–5899

David C. Tully\*, Agnès Vidal, Arnab K. Chatterjee, Jennifer A. Williams, Michael J. Roberts, H. Michael Petrassi, Glen Spraggon, Badry Bursulaya, Reynand Pacoma, Aaron Shipway, Andrew M. Schumacher, Henry Danahay, Jennifer L. Harris

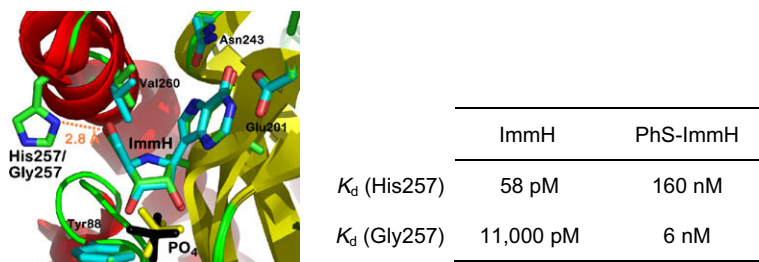


Structure-based design was utilized to guide the early stage optimization of a substrate-like inhibitor to afford potent peptidomimetic inhibitors of the channel-activating protease prostatic. The first X-ray structure of a small molecule inhibitor bound to the active site of prostatic is also reported.

**Immucillins in custom catalytic-site cavities**

pp 5900–5903

Andrew S. Murkin, Keith Clinch, Jennifer M. Mason, Peter C. Tyler, Vern L. Schramm\*

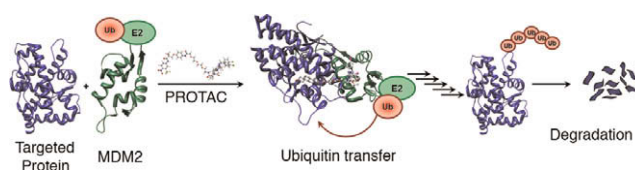


Neighboring-group participation in the reaction catalyzed by purine nucleoside phosphorylase involves His257-facilitated compression of the 5'- and 4'-ribose oxygens. The His257Gly mutant opens a space for preferential binding of 5'-substituted Immucillins, transition-state analogues of this reaction.

**Targeted intracellular protein degradation induced by a small molecule: En route to chemical proteomics**

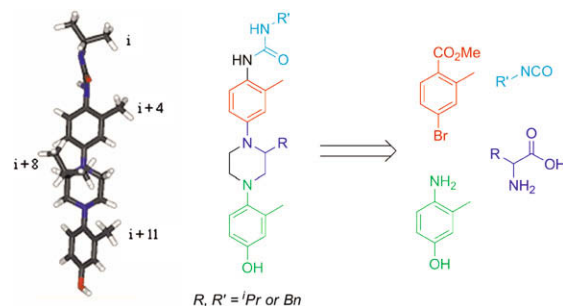
pp 5904–5908

Ashley R. Schneekloth, Mathieu Pucheault, Hyun Seop Tae, Craig M. Crews\*

**Synthesis of  $\alpha$ -helix mimetics with four side-chains**

pp 5909–5911

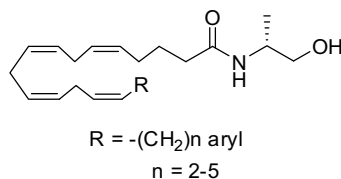
Per Restorp, Julius Rebek Jr.\*



**Development of novel tail-modified anandamide analogs**

pp 5912–5915

Fenmei Yao, Chen Li, Subramanian K. Vadivel, Anna L. Bowman, Alexandros Makriyannis \*

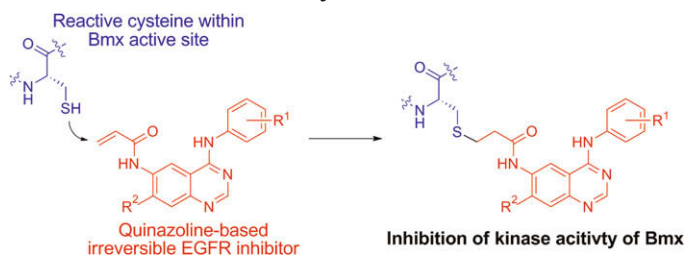


Synthesis and evaluation of a series of anandamide analogs of variable chain lengths in which the terminal carbon is functionalized with a phenyl, substituted phenyl or heterocyclic group.

**Clinical stage EGFR inhibitors irreversibly alkylate Bmx kinase**

pp 5916–5919

Wooyoung Hur, Anastasia Velentza, Sungjoon Kim, Laura Flatau, Xinnong Jiang, David Valente, Daniel E. Mason, Melissa Suzuki, Brad Larson, Jianming Zhang, Anna Zagorska, Michael DiDonato, Advait Nagle, Markus Warmuth, Steven P. Balk, Eric C. Peters, Nathanael S. Gray \*



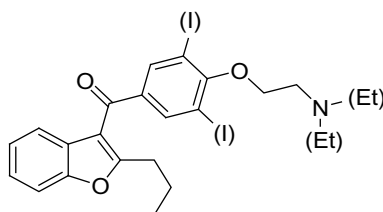
Quinazoline-based clinical irreversible EGFR inhibitors is found to inhibit Tec-family kinase Bmx by covalent modification of reactive cysteine residue within active site.

**Trace amine-associated receptor 1 (TAAR<sub>1</sub>) is activated by amiodarone metabolites**

pp 5920–5922

Aaron N. Snead, Motonori Miyakawa, Edwin S. Tan, Thomas S. Scanlan \*

Amiodarones

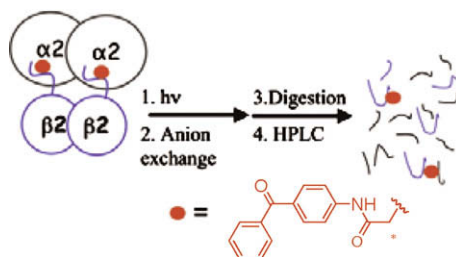


We report here the synthesis and characterization of a panel of potential amiodarone metabolites that have significant structural similarity to thyroid hormone and its metabolites, the iodothyronamines. Several of these amiodarone derivatives act as specific agonists of the G protein-coupled receptor (GPCR) trace amine-associated receptor 1 (TAAR<sub>1</sub>).

**Mapping the subunit interface of ribonucleotide reductase (RNR) using photo cross-linking**

pp 5923–5925

A. Quamrul Hassan, JoAnne Stubbe \*



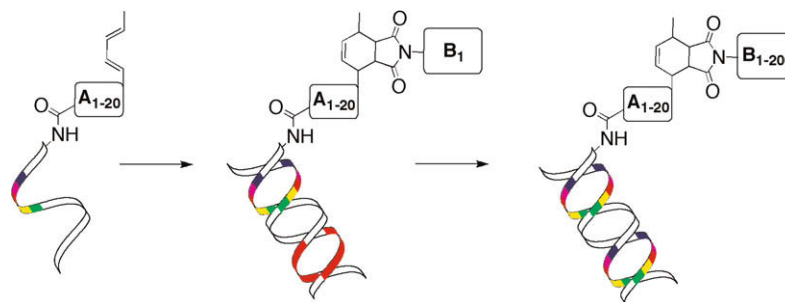
Molecular insight into the subunit interface of *Escherichia coli* RNR using peptide mapping is presented.



**Design and synthesis of a novel DNA-encoded chemical library using Diels-Alder cycloadditions**

pp 5926–5931

Fabian Buller, Luca Mannocci, Yixin Zhang, Christoph E. Dumelin, Jörg Scheuermann, Dario Neri\*

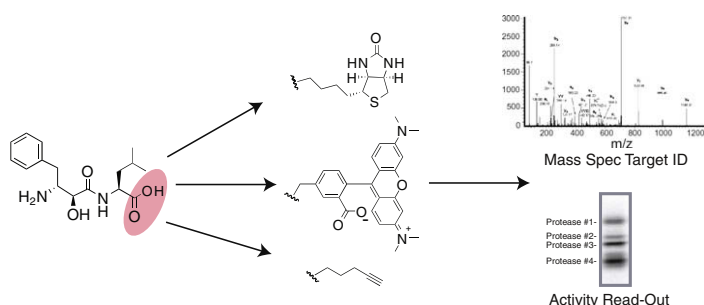


Synthesis and characterization of a novel 4000 compound DNA-encoded chemical library based on the Diels-Alder cycloaddition reaction.

**Development of bestatin-based activity-based probes for metallo-aminopeptidases**

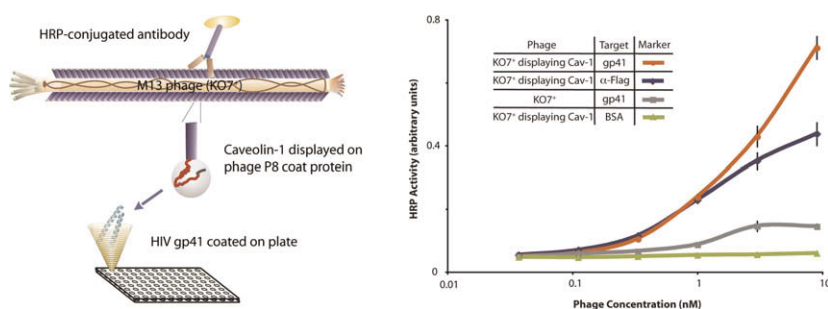
pp 5932–5936

Michael B. Harbut, Geetha Velmourougane, Gilana Reiss, Rajesh Chandramohanadas, Doron C. Greenbaum\*

**Phage display of functional, full-length human and viral membrane proteins**

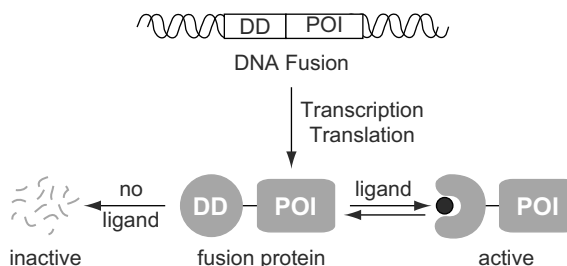
pp 5937–5940

Sudipta Majumdar, Agnes Hajduczki, Aaron S. Mendez, Gregory A. Weiss\*

**Recent progress with FKBP-derived destabilizing domains**

pp 5941–5944

Bernard W. Chu, Laura A. Banaszynski, Ling-chun Chen, Thomas J. Wandless\*



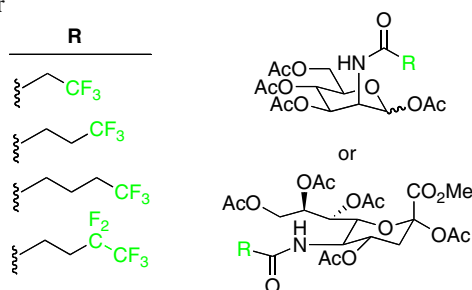
We recently engineered mutants of the FKBP12 protein that are rapidly degraded when expressed in cells. Recent results expand the utility of this general technology to provide small molecule control over protein stability.



### Fluorination of mammalian cell surfaces via the sialic acid biosynthetic pathway

pp 5945–5947

Laila Dafik, Marc d'Alarcao\*, Krishna Kumar\*



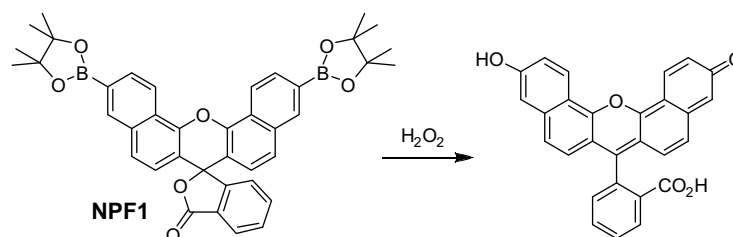
The surfaces of living cells have been fluorinated by incubation with *N*-fluoroacyl mannosamines or *N*-fluoroacyl neuraminic acids. Fluorinated cells showed reduced adhesion to extracellular matrix biomolecules.



### A red-emitting naphthofluorescein-based fluorescent probe for selective detection of hydrogen peroxide in living cells

pp 5948–5950

Aaron E. Albers, Bryan C. Dickinson, Evan W. Miller, Christopher J. Chang\*



The synthesis, spectroscopy, and live-cell evaluation of a red-emitting fluorescent probe for cellular hydrogen peroxide are reported.

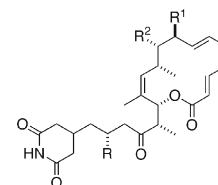


### Evaluation of new migrastatin and dorrigocin congeners unveils cell migration inhibitors with dramatically improved potency

pp 5951–5954

Jianhua Ju, Scott R. Rajski, Si-Kyu Lim, Jeong-Woo Seo, Noël R. Peters, F. Michael Hoffmann, Ben Shen\*

Biological evaluation of new cell migration inhibitors bearing migrastatin (MGS)-derived scaffolds is reported unveiling structural elements crucial to activity and two new MGS analogs with superior activity.

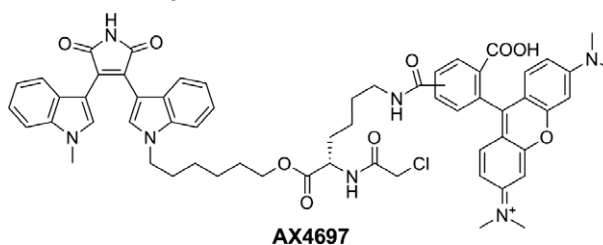


MGS: R = H, R<sup>1</sup> = OCH<sub>3</sub>, R<sup>2</sup> = OH  
 14: R = OH, R<sup>1</sup> = OCH<sub>3</sub>, R<sup>2</sup> = OH  
 17: R = OH, R<sup>1</sup> = R<sup>2</sup> = H  
 Cell migration inhibitor potency:  
 17 >> 14 > MGS

### Design and synthesis of AX4697, a bisindolylmaleimide exo-affinity probe that labels protein kinase C alpha and beta

pp 5955–5958

Yongsheng Liu, Jiangyue Wu, Helge Weissig, Juan M. Betancort, Wen Zhi Gai, Phillip S. Leventhal, Matthew P. Patricelli, Babak Samii, Anna K. Szardenings, Kevin R. Shreder\*, John W. Kozarich\*



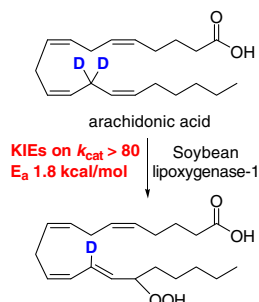
The synthesis and biochemical characterization of **AX4697**, bisindolylmaleimide-derived, exo-affinity probe for PKCα and β, is described.



**Kinetic isotope effects in the oxidation of arachidonic acid by soybean lipoxygenase-1**

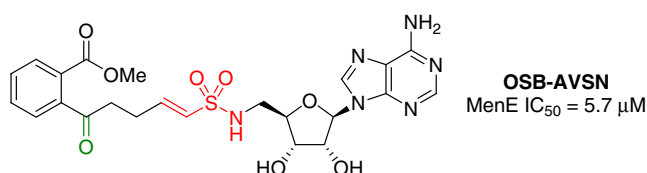
pp 5959–5962

Cyril Jacquot, Sheng Peng, Wilfred A. van der Donk\*

**Mechanism-based inhibitors of MenE, an acyl-CoA synthetase involved in bacterial menaquinone biosynthesis**

pp 5963–5966

Xuequan Lu, Huaning Zhang, Peter J. Tonge\*, Derek S. Tan\*

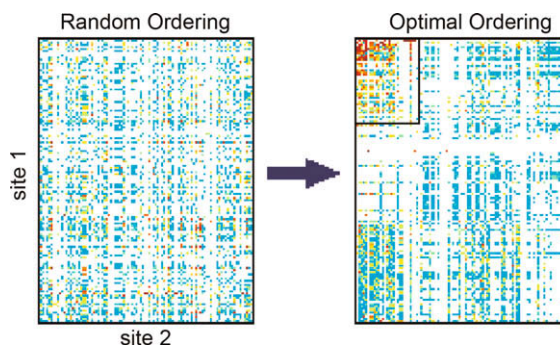


The design, synthesis, and biochemical evaluation of mechanism-based OSB-CoA synthetase inhibitors is reported.

**Descriptor-free molecular discovery in large libraries by adaptive substituent reordering**

pp 5967–5970

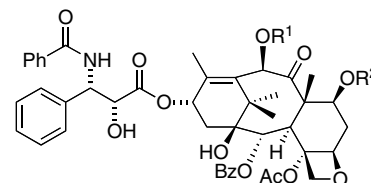
Scott R. McAllister, Xiao-Jiang Feng\*, Peter A. DiMaggio Jr., Christodoulos A. Floudas\*, Joshua D. Rabinowitz, Herschel Rabitz\*

**Paclitaxel succinate analogs: Anionic and amide introduction as a strategy to impart blood–brain barrier permeability**

pp 5971–5974

Brandon J. Turunen, Haibo Ge, Jariat Oyetunji, Kelly E. Desino, Veena Vasandani, Sarah Güthe, Richard H. Himes, Kenneth L. Audus, Anna Seelig, Gunda I. Georg\*

TX-67 (C10 hemi-succinate) analogs were investigated, including C7 regioisomers, esters, amides, and one-carbon homologs for tubulin stabilization, cytotoxicity, and Pgp interactions. All carboxylic acid analogs and several of the amides had no apparent interactions with Pgp, whereas the ester variants displayed characteristics of Pgp substrates. Furthermore, it was demonstrated that hydrogen-bonding properties were significant with respect to Pgp interactions.

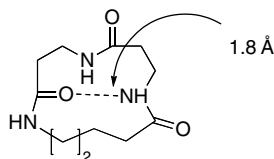


**Series A:**  $R^1$  = hemi-succinate and glutarate, methyl ester, amides;  $R^2$  = H  
**Series B:**  $R^1$  = Ac;  $R^2$  = hemi-succinate and glutarate, methyl ester, amides

**Synthesis and structural study of cyclic 5-aminovaleric acid-linked  $\beta$ -Ala- $\beta$ -Ala dipeptides**

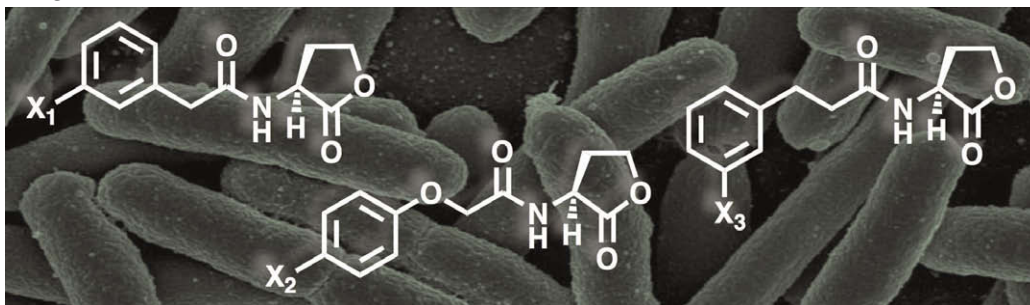
pp 5975–5977

Anne Mengel, Oliver Reiser, Jeffrey Aubé\*

**Evaluation of a focused library of *N*-aryl L-homoserine lactones reveals a new set of potent quorum sensing modulators**

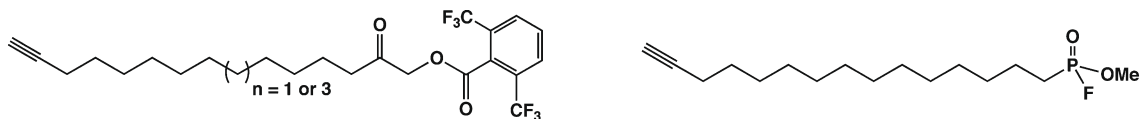
pp 5978–5981

Grant D. Geske, Margrith E. Mattmann, Helen E. Blackwell\*

**Chemical probes for profiling fatty acid-associated proteins in living cells**

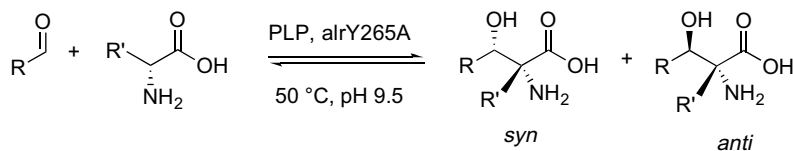
pp 5982–5986

Anuradha Raghavan, Guillaume Charron, James Flexner, Howard C. Hang\*

**Fatty acid-based chemical probes****Synthesis of  $\beta$ -hydroxy- $\alpha$ -amino acids with a reengineered alanine racemase**

pp 5987–5990

Kateryna Fesko, Lars Giger, Donald Hilvert\*



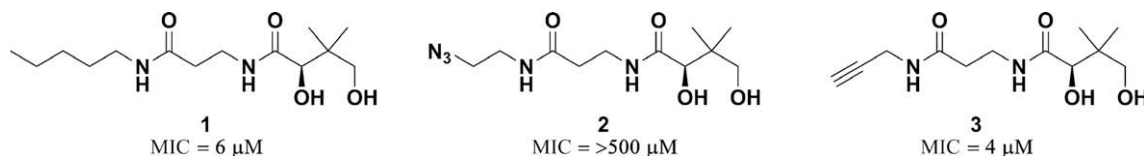
The Y265A mutant of alanine racemase catalyzes the stereoselective condensation of glycine or alanine with a range of aromatic aldehydes.



**Antibiotic evaluation and in vivo analysis of alkynyl Coenzyme A antimetabolites in *Escherichia coli***

pp 5991–5994

Andrew C. Mercer, Jordan L. Meier, Gene H. Hur, Andrew R. Smith, Michael D. Burkart\*

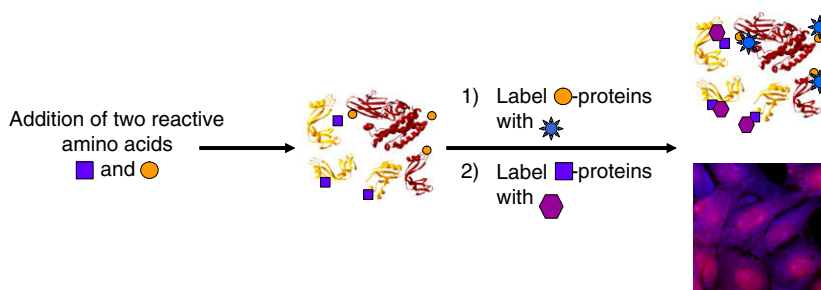


A panel of pantetheine analogues was synthesized and the mechanism of their differential activity against *Escherichia coli* was probed with a series of kinetic and in vivo assays. The results have implications on the purported mode of action of this class of antibiotics.

**Two-color labeling of temporally defined protein populations in mammalian cells**

pp 5995–5999

Kimberly E. Beatty, David A. Tirrell\*

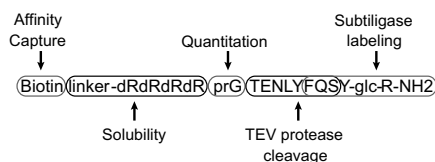


Homopropargylglycine and azidohomoalanine have been used to label newly synthesized proteins in mammalian cells.

**Tags for labeling protein N-termini with subtiligase for proteomics**

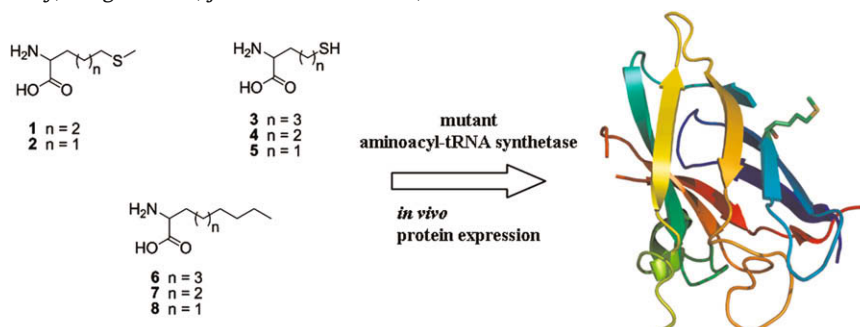
pp 6000–6003

Hikari A. I. Yoshihara, Sami Mahrus, James A. Wells\*

**A promiscuous aminoacyl-tRNA synthetase that incorporates cysteine, methionine, and alanine homologs into proteins**

pp 6004–6006

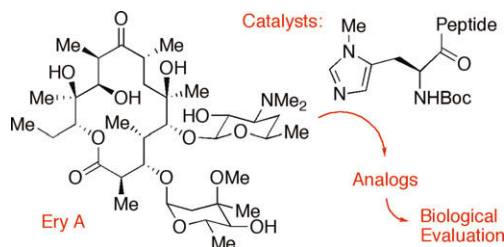
Eric Brustad, Mark L. Bushey, Ansgar Brock, Johnathan Chittuluru, Peter G. Schultz\*



## Catalytic site-selective synthesis and evaluation of a series of erythromycin analogs

pp 6007–6011

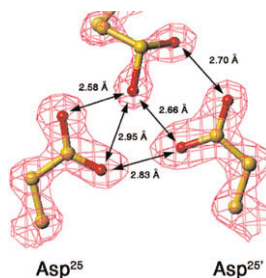
Chad A. Lewis, Janie Merkel, Scott J. Miller\*



## Reprint of "Crystal structure of chemically synthesized HIV-1 protease and a ketomethylene isostere inhibitor based on the p2/NC cleavage site" [Bioorg. Med. Chem. Lett. 18 (2008) 4554–4557]

pp 6012–6015

Vladimir Yu. Torbeev\*, Kalyaneswar Mandal, Valentina A. Terechko, Stephen B. H. Kent



Crystal structure of HIV-1 protease with its ketomethylene isostere inhibitor is reported.

## OTHER CONTENTS

## Instructions to contributors

p I

\*Corresponding author

Supplementary data available via ScienceDirect

## COVER

The Cravatt lab develops advanced synthetic and analytical chemistry technologies for the proteome-wide analysis of enzyme function. Shown are exemplary activity-based chemical probes (stick diagram), enzyme activity proteomic profiles (red bands in backdrop), and metabolomic signatures arising from enzyme inhibition (blue heat diagram) that collectively represent several of the core technologies introduced by the Cravatt group. [Hoover, H. S., Blankman, J. L., Niessen, S., Cravatt, B. F. *Bioorg. Med. Chem. Lett.* **2008**, 18, 5838.]

Indexed/Abstracted in: Beilstein, Biochemistry & Biophysics Citation Index, CANCERLIT, Chemical Abstracts, Chemistry Citation Index, Current Awareness in Biological Sciences/BIOBASE, Current Contents: Life Sciences, EMBASE/Excerpta Medica, MEDLINE, PASCAL, Research Alert, Science Citation Index, SciSearch, TOXFILE



ISSN 0960-894X